Received: 5 March 2018 | Accepted: 2 July 2018
DOI: 10.1002/pcr2.10020

WILEY Polymer Crystallization

FULL PAPER

Non-isothermal crystallization of poly(ε-caprolactone) nanocomposites with soy lecithin-modified bentonite

Danila Merino[1] | **Vera Alejandra Alvarez**[1] | **Claudio Javier Pérez**[2]

[1]Grupo Materiales Compuestos Termoplásticos (CoMP) Instituto de Investigaciones en Ciencia y Tecnología de Materiales (INTEMA), Facultad de Ingeniería, Universidad Nacional de Mar del Plata (UNMdP) and Consejo Nacional de Ciencia y Tecnología de Materiales (CONICET), Buenos Aires, Argentina

[2]Grupo Ciencia e Ingeniería de Polímeros, Instituto de Investigaciones en Ciencia y Tecnología de Materiales (INTEMA), Facultad de Ingeniería, Universidad Nacional de Mar del Plata (UNMdP) and Consejo Nacional de Ciencia y Tecnología de Materiales (CONICET), Buenos Aires, Argentina

Correspondence
Claudio Javier Pérez, Grupo Ciencia e Ingeniería de Polímeros, Instituto de Investigaciones en Ciencia y Tecnología de Materiales (INTEMA), Facultad de Ingeniería, Universidad Nacional de Mar del Plata (UNMdP) and Consejo Nacional de Ciencia y Tecnología de Materiales (CONICET), Colón 10890, Mar del Plata 7600, Buenos Aires, Argentina.
Email: cjperez@fi.mdp.edu.ar

Funding information
National Agency Promotion Scientific and Technological (ANPCyT); National Research Council of Argentina (CONICET)

Non-isothermal crystallization behavior of poly(ε-caprolactone)/bentonite (natural and soy lecithin-modified) nanocomposites was studied by means of differential scanning calorimetry (DSC). In addition, a microscopic analysis of cryofracture surface was performed by scanning electron microscopy (SEM). Experimental data show that pure bentonite (Bent) acts as retarding agent and that soy lecithin partially counteracts this effect because it accelerates the crystallization process. The soy lecithin was used as natural and cheap clay modifier that can be used in food contact applications, which is the thought application for the studied materials. Kinetic parameters, obtained by using classical methods such as Avrami and Mo models, were able to partially describe the non-isothermal crystallization behavior of the studied materials and the results are further supported by the effective activation energy calculations by iso-conversional method of Friedman. The full models, which take into account the different parameters during cooling under non-isothermal conditions, were used to construct continuous cooling transformations (CCTs) diagrams that confirm all previous results and that will be used to determine the processing conditions of studied materials.

KEYWORDS
bentonite, biodegradable polymer, non-isothermal crystallization, polycaprolactone

1 | INTRODUCTION

The global consumption of biodegradable polymers has increased due to their potential applications in the field of environmental benign plastic products. Especially the push toward the bio-based economy and greener society has impulse the development of new bio-based materials.[1] A vast variety of biodegradable polymers have been prepared and several of them have been industrialized, such as chitin, chitosan, poly(β-hidroxybutyrate), or poly(ε-caprolactone) (PCL). These materials have a great market that includes packaging materials, hygiene products, consumer goods, and agricultural tools. In order to improve their performance, they could be filled with different inorganic synthetic and or natural compounds in order to increase several properties, such as mechanical and impact properties and decrease others such as gas permeability.[2–4]

Particularly, in recent years, PCL has been widely used in the preparation of blends with other biodegradable polymers such as polylactic acid and thermoplastic starch,[5,6] or as matrix for nanocomposites preparation using natural fillers such as starch nanoparticles,[7] carbon nanotubes,[8] nanoclays,[9] or cellulose nanocrystals.[10] Among them, the use of nanoclay as reinforcement is highlighted thanks to the proven improvements in relevant application properties. Such improvements are mainly obtained with low clay content, usually below 5 wt. %, and are related with thermomechanical and barrier properties and also with the rate of polymer biodegradation. This enhanced performance of nanocomposites is a result of the large

https://doi.org/10.1002/pcr2.10020

number of interactions between both components, matrix and clay, coming from the high surface area of nanometric-sized silicate layers, thin and homogeneously dispersed in the polymer matrix.[11] It is interesting to note that most of the published work on PCL/clays nanocomposites use ammonium salts to modify the clay and introduces limitations for their use in food contact applications. In a previous work, we reported the chemical modification of bentonite (Bent) with a cheap natural product, soy lecithin (SL), and the effect that this modification produced on the final properties of PCL/clay nanocomposites.[12] In that work, it was found that the nanocomposites presented intercalated-exfoliated structures and those results were supported by the decrease on the water vapor permeability by the addition of SL-modified bentonite to the neat PCL. However, melt rheology, differential scanning calorimetry (DSC), and mechanical tensile tests yielded unexpected results suggesting the decrease in the molecular weight of the PCL matrix being higher as a function of SL content.

During the last decade, many studies related to the crystallization of PCL nanocomposites have been published,[13–22] and they have shown controversial results regarding the nucleating or retarding effect of PCL modified with several compounds: pure carbon nanotubes and/or functionalized with different chemical agents,[13–15] cellulose,[16,17] organoclays,[18] and bamboo fiber.[19] The effects have been studied analyzing different experimental parameters as the changes on the crystallization temperature (increase or decrease), the crystallization rate (higher or lower), the effective energy barrier (increase or reduction), or the half-crystallization time (decrease or increase). In the previous studies, both effects (retarding or accelerating ones) were also demonstrated by the use of different theoretical models, such as Osawa, Avrami, or Mo.

The aim of this work was to study and to model the non-isothermal crystallization process of PCL reinforced with different contents of SL-modified bentonite. The effect of the Bent concentration and the SL/Bent ratios on the modified clay will also be analyzed by the application of theoretical models. The behavior of these materials during non-isothermal crystallization from the molten state is of increasing technological importance because real industrial processes such as extrusion and film forming usually proceed under dynamic non-isothermal conditions. Moreover, from scientific point of view, the study of crystallization in dynamic conditions may expand the general understanding of crystallization behavior of polymers as many isothermal methods are often restricted to a narrow temperature range.[20,21]

2 | EXPERIMENTAL

2.1 | Materials

PCL, CAPA FB 100, with Mw = 100 000 g/mol was purchased from Perstorp (Sweden). The Bent, with a cation exchange capacity of 105 mequiv/100 g, was provided by Minarmco S.A. (Argentina). SL was supplied by Melar S.A. (Argentina). All materials were used as received.

2.2 | Nanoclays preparation

As it has been reported in our previous work,[22] three SL-modified bentonites were prepared to be used as fillers of PCL. Briefly, a Bent dispersion was mixed with a SL solution, heated at 75°C and stirred for 2 hours. Nanoclays were obtained by using the SL/Bent ratios of 0.25, 0.50, and 1 and were labeled as A, B, and C, respectively.

2.3 | PCL nanocomposites preparation

PCL nanocomposites reinforced with 1 and 2 wt. % of Bent, A, B, and C nanoclays were prepared as reported in our previous work.[12] In short, nanocomposites were obtained using a two counter-rotating roller rotors-Brabender type mixer at 100°C for 10 minutes. Then, sheets of 1 mm thickness were obtained by hot-pressing for 10 minutes at 100°C and 75 kg/cm^2. Nanocomposites were labeled indicating the clay content and type. For example, "PCL + 1%A" is the nanocomposite from PCL and 1 wt. % of A nanoclay.

2.4 | Characterization methods

2.4.1 | Morphological characterization

The morphology of Bent, A, B, and C clays/PCL nanocomposites on a microscopic scale was examined using scanning electron microscopy (SEM Philips model JEOL JSM-6460 LV). PCL and its nanocomposites were cooled in liquid air and then broken into two pieces. Then, the cut specimens were fixed with silicon adhesive onto small glass pieces. Finally, cryofractured surfaces were covered with a thin layer of gold. The scanning electron micrographs were reordered at 1000× of magnification.

2.4.2 | Non-isothermal crystallization process

The non-isothermal crystallization process was studied by means of a DSC (Perkin Elmer 7). Samples of about 10 mg were accurately weighted. A first run was done from room temperature to 110°C at a heating rate of 10°C/min. Then, the samples were kept for 5 minutes at 110°C in order to allow the complete melting of the crystals and to remove the thermal history. After that, the samples were cooled to room temperature at different cooling rates: 5, 10, 15, 20, and 30°C/min. All DSC analyses were performed under nitrogen atmosphere.

3 | RESULTS AND DISCUSSION

3.1 | Systems characterization

The preparation and characterization of A, B, and C nanoclays were reported in our previous work.[12] The obtained main results suggested that the organic contents present in nanoclays were 16.2 ±0.2%, 22.8 ±0.2%, and 41.9 ±0.4% for A, B, and C, respectively, and that the SL was intercalated between clay sheets and also adsorbed onto the platelet edges and faces. Increments in interlamellar spacing were observed as SL content increases. In addition, we found that the thermal stability of nanoclays decreases as a function of SL content, and those nanoclays were not affected during processing of PCL nanocomposites performed at 100°C. Finally, SL-modified nanoclays presented an important moisture content reduction when compared with Bent, thus improving the interaction with the highly hydrophobic PCL matrix. Once incorporated into PCL matrix, nanocomposite characterization by X-ray diffraction analysis[12] suggested that intercalated-exfoliated structures were obtained. Particularly, nanocomposites with Bent, A, and B presented an intercalated structure, while those with C presented an intercalated-exfoliated one. However, melt rheology results exhibited evidences of thermal degradation of the matrix.

In order to assess the state of dispersion of different used clays (Bent, A, B, and C) on PCL matrix, SEM micrographs of cryofractured surfaces of nanocomposites were taken. Figure 1 shows SEM micrographs of PCL and its nanocomposites with 1% and 2% of Bent, A, B, and C. Figure 1A shows the cryofracture surface of the pure PCL. No aggregates were present on its surface. Figure 1B,C shows the surface of nanocomposites with Bent. In this case, the presence of clay agglomerates can be observed, being greater when the clay content is 2%. White arrows were included in the figure to mark the agglomerates. The remaining figures (Figure 1D-I) show that organoclays A, B, and C displayed a good degree of dispersion in PCL as no aggregates were observed with the micrometric magnification utilized. This result suggests that the chemical modification of Bent increases the compatibility with PCL matrix promoting strong interactions between the filler and the polymeric chains. Therefore, the analysis has revealed that Bent modification can provide a useful method to prepare nanocomposites with a fine dispersion of the reinforcement and a good adhesion.

3.2 | Non-isothermal crystallization process

The degree of crystallinity of each material was calculated from the following equation[23]:

$$X_{\mathrm{cr}}(\%) = \frac{\Delta H_f}{w_{\mathrm{PCL}} \times \Delta H_{100}} \times 100 \tag{1}$$

where ΔH_f is the experimental heat of fusion, w_{PCL} is the weight fraction of PCL, and ΔH_{100} is the heat of fusion of 100% crystalline PCL; 136 J/g.[24]

Figure 2 shows the crystallization behavior of pure polymer and nanocomposites at a cooling rate of 10°C/min. The crystallization temperatures and the degree of crystallinity were extracted from the curves and the obtained values are summarized in Table 1.

It can be observed that the degree of crystallinity decreased with the incorporation of unmodified bentonite (1% and 2%). A similar decreasing trend was reported by other authors[4,25] and it was attributed to the hindering of the polymer chain mobility, and effective diffusion of chains to the growing fronts of crystallites is impeded by the nanoclay. The limited crystal growth produces crystallites with reduced grain size and lowers the degree of crystallinity. The decrease in crystallinity may further be attributed to the polymer–clay interactions.[4] On one hand, the crystallinity increase with SL content, indicating that SL acts as nucleating agent for the crystallization of PCL.[26,27]

On the other hand, it is possible to observe that the crystallization temperature of PCL slightly decreased with the incorporation of pure bentonite, delaying the crystallization process. This phenomenon could be probably related to the presence of more heterogeneous nucleation sites to reduce the perfection of PCL crystallite in the nanocomposite.[4,28,29]

An approximation of the crystallization rate can be made by calculating the overall crystallization rate (OCR) ($t_{1/2}{}^{-1}$), where $t_{1/2}$ (half-crystallization time) is the time at which the relative degree of crystallinity approaches to 0.5. This parameter is proportional to both the primary nucleation rate and the crystal growth.[30] It is important to say that a lower value for OCR ($t_{1/2}{}^{-1}$) indicates slower crystallization.

Figure 3 shows the experimental OCR as a function of cooling rate for PCL and nanocomposites with 1% of each clay (Figure 3A) and (Figure 3B) PCL and nanocomposites with 2% of each clay.

As expected, the values of OCR increased with the increased cooling rate for all materials[31,32] due to a higher driving force process. From the figure, it can be observed that, for a fixed cooling rate, the OCR decreased when Bent (1% and 2%) was incorporated, indicating that the addition of Bent makes the crystallization process slower (retarding effect). On the other hand, the OCR increased with the modified nanoclays (with respect to PCL/unmodified bentonite nanocomposites) which could be related with an improved interaction of the SL with PCL, due to higher compatibility but also with the fact that SL acts as an accelerating agent on the crystallization process. The effect was more notorious in Figure 3A. The greater bentonite content in Figure 3B does not allow appreciating the differences between the different content of SL.

3.3 | Modeling of non-isothermal crystallization process

Avrami's equation has been widely applied for the non-isothermal crystallization of polymers.[33–35] It assumes that the relative degree of crystallinity develops with the crystallization time t[36]

$$\alpha = 1 - \exp(-Z_t t^n) \tag{2}$$

where n is the Avrami crystallization exponent dependent on the mechanism of nucleation, α is the relative degree of crystallinity at time t, and Z_t is a polymer or blend rate constant involving both nucleation and growth rate parameters.[34] Considering the non-isothermal character of the process, Jeziorny pointed out that the value of rate parameter Z_t should be adequately corrected.[37] Assuming approximately constant the cooling rate (φ), the final form of the parameter characterizing the kinetics of non-isothermal crystallization can be expressed as follows:

$$\ln Z_c = \frac{\ln Z_t}{\emptyset} \tag{3}$$

The parameters of Avrami equation were obtained by using a typical nonlinear Levenberg–Marquard regression method in the Origin software, in the range of α between 0.01 and 0.4. The Avrami approach was applied to the early stages of crystallization to avoid complications arise from the effects of secondary crystallization process. Figure 4 shows a relative degree of crystallinity (α) as a function of time for PCL + 1% B. Red lines show the range adjusted with the regression method and in all analyzed materials the adjustment was adequate (R^2 > 0.9900). The obtained parameters are summarized in Table 2.

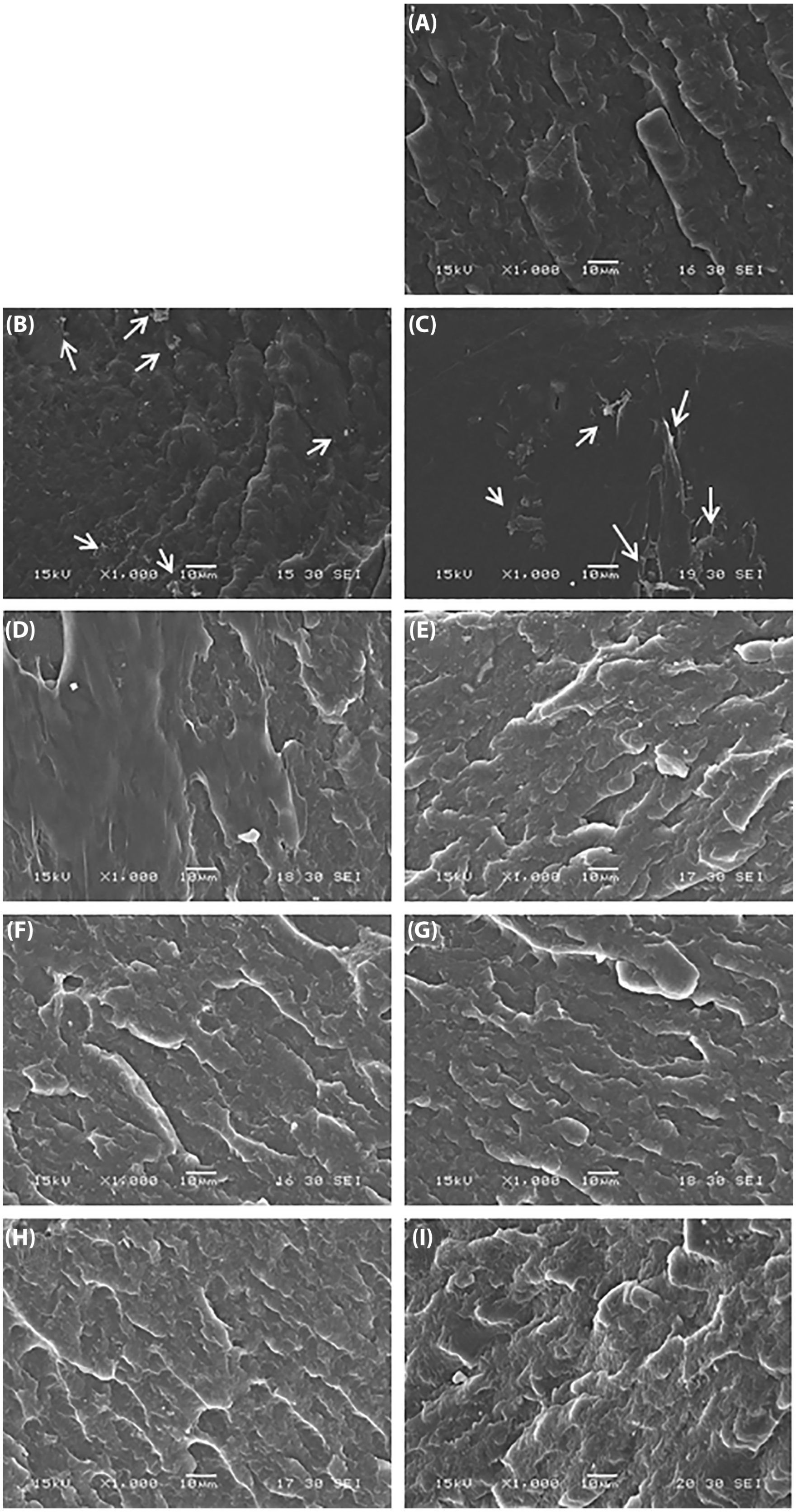

FIGURE 1 SEM micrographs of A, PCL; B, PCL + 1% Bent; C, PCL + 2% Bent; D, PCL + 1% A; E, PCL + 2% A; F, PCL + 1% B; G, PCL + 2% B; H, PCL + 1% C; and I, PCL + 2% C

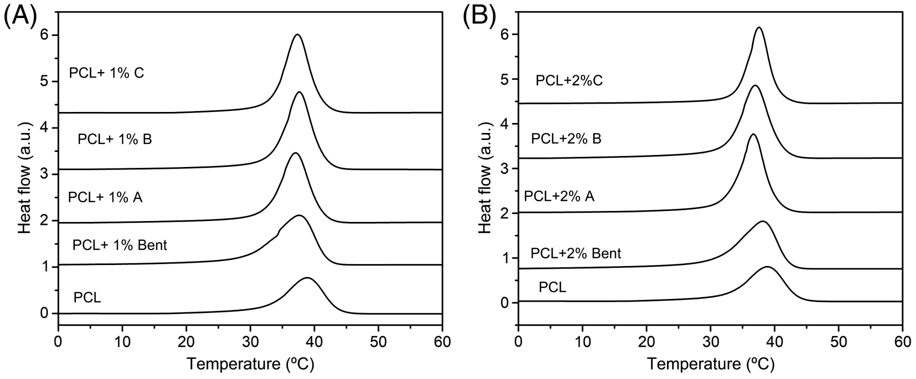

FIGURE 2 Non-isothermal crystallization curves obtained at a cooling rate of 10 °C/min. A, PCL and nanocomposites with 1% of each clay and B, PCL and nanocomposites with 2% of each clay

TABLE 1 Parameters of non-isothermal crystallization for different materials studied at 10°C/min

Sample	T_c (°C)	X (%)
PCL	38.9	44.0
PCL + 1% Bent	38.6	42.3
PCL + 1% A	38.2	43.3
PCL + 1% B	37.6	45.5
PCL + 1% C	37.3	49.9
PCL + 2% Bent	38.5	43.0
PCL + 2% A	37.3	44.5
PCL + 2% B	37.0	46.8
PCL + 2% C	37.5	50.0

It is possible to observe that Z_c increased as a function of cooling rate.[32,35,38] On the other hand, for a fixed cooling rate, *n* decreased when Bent was incorporated to PCL matrix and that, in general, increases with the content of SL, with some exceptions. The opposite behavior was observed with the parameter Z_c. This is concordant with the retardant effect produced by the pure bentonite.[35,39] It is important to remark that this model does not show appreciable differences between the different blends studied.

The overall non-isothermal crystallization kinetics of pure PCL and nanocomposites with SL was also studied using the Mo's formalism,[40] which is a combination of Avrami and Ozawa equations. This is based on the following equation:

$$\ln \emptyset = \ln F(T) - a \ln t \tag{4}$$

where $F(T) = [K(T)^{*}Z_t^{-1}]^{m-1}$ refers to the cooling rate, which has to be chosen at unit crystallization time when the measured system amounts to a certain degree of crystallinity; *a* is the ratio of the Avrami exponent *n* to the Ozawa exponent *m*, (*n*/*m*).

Perfect linear relationship between ln φ and ln *t* can be obtained. An example is shown in Figure 5 (PCL + 1% B). A similar behavior was observed for all studied systems. This gives the idea that apparently, non-isothermal crystallization analysis by Mo's method is suitable for studied materials.

The kinetic parameter *F*(*T*), obtained from slope, and *a*, from intercept, are listed in Table 3. As it was previously indicated, values between 20% and 40% of relative crystallinity were considered. It can be observed, for all systems, that *a* and *F*(*T*) values slightly changed with the relative degree of crystallinity. On the other hand, at a given degree of crystallinity, *F*(*T*) increases with the incorporation of pure Bent (1% and 2%) indicating that Bent acts as retarding agent[35,38] and then decreases for modified one, also with the SL content, in accordance with other results that show that SL acts as accelerating of the crystallization process. The *a* values are in the range 1.4-1.7.

3.4 | Nucleation activity

Nucleation activity (φ) is a measurement of the decrease of the three dimensional nucleation with the addition of reinforcement.[41] If the

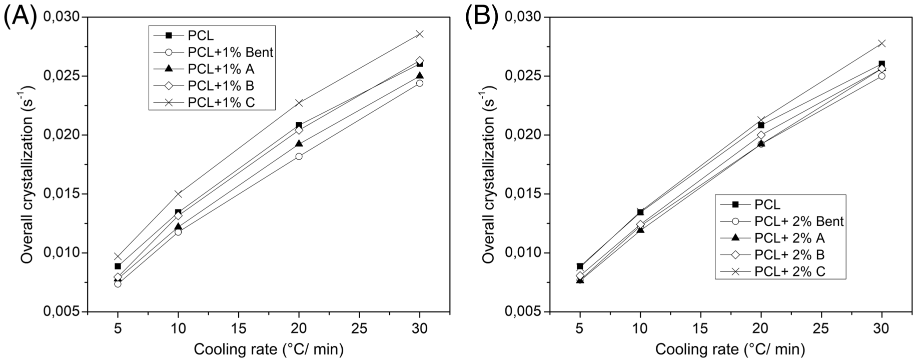

FIGURE 3 Overall crystallization as a function of cooling rate for A, PCL and nanocomposites with 1% of each clay and B, PCL and nanocomposites with 2% of each clay

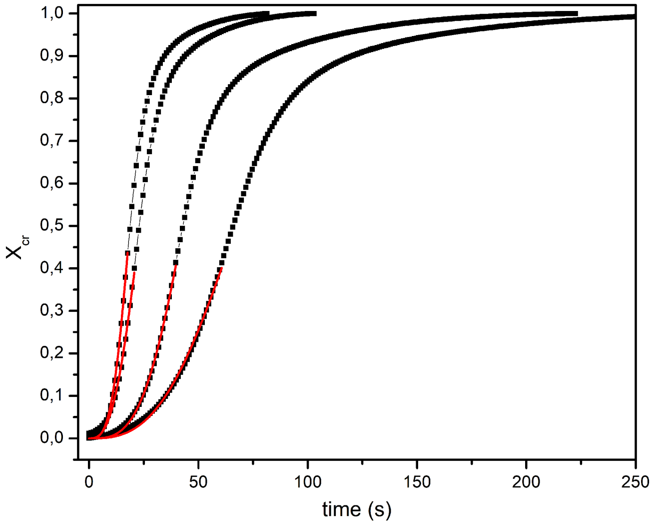

FIGURE 4 Relative crystallization as a function of time for crystallization of PCL + 1% B

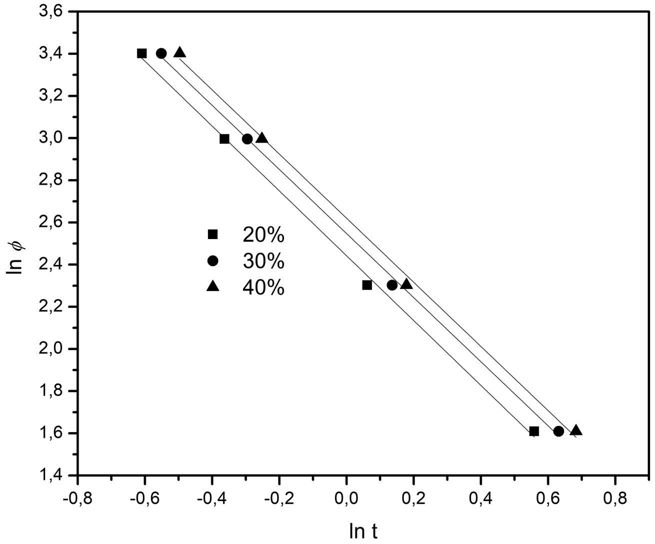

FIGURE 5 Ln ϕ versus log t from the Mo's equation for non-isothermal crystallization of PCL + 1% B

TABLE 3 Mo's parameters for the non-isothermal of pure PCL and nanocomposites

Crystallinity (%)	20		30		40	
Samples	*a*	*F(T)*	*a*	*F(T)*	*a*	*F(T)*
PCL	1.73	2.27	1.71	2.43	1.69	2.55
PCL + 1% Bent	1.60	2.50	1.59	2.62	1.57	2.73
PCL + 1% A	1.55	2.52	1.53	2.62	1.52	2.70
PCL + 1% B	1.54	2.44	1.52	2.55	1.52	2.62
PCL + 1% C	1.60	2.26	1.59	2.38	1.59	2.47
PCL + 2% Bent	1.58	2.43	1.59	2.56	1.54	2.67
PCL + 2% A	1.40	2.51	1.42	2.62	1.45	2.70
PCL + 2% B	1.53	2.46	1.54	2.57	1.55	2.66
PCL − 2% C	1.59	2.40	1.57	2.49	1.55	2.55

reinforcement is extremely active, the nucleation activity will tend to zero, while for inert reinforcement, it will be close to one.[41] For nucleation from the melt, the cooling rate is represented by Equation 5, at temperatures close to melting:

$$\ln\emptyset = A - \frac{B}{\Delta T_c^2} \tag{5}$$

where φ is the cooling rate, A is a constant, $\Delta T_c = T_m - T_c$ is the degree of under cooling, T_c is the crystallization temperature, T_m is the melting temperature, and B is the parameter related to the three dimensional nucleation. φ can be calculated from the following equation:

$$\varphi = \frac{B^*}{B} \tag{6}$$

where B is the parameter for the pure polymer and B^* for the nanocomposites, and they were obtained from Equation 5. Table 4 shows the calculated values of the activity nucleation of the studied systems. It is clear that the values are lower in the systems that contain SL (higher nucleating effect), without appreciable difference between 1% and 2% Bent.

As it was described above, the crystallization temperature depends on the cooling rate. For non-isothermal crystallization, it is also interesting to evaluate the effective energy barrier, ΔE. The differential isoconversional method of Friedman[42] is one of most appropriate methods for evaluating the effective energy barrier:

$$\ln\left(\frac{\partial\alpha}{\partial t}\right) = \text{constant} - \frac{\Delta E_x}{RT} \tag{7}$$

where $\partial\alpha/\partial t$ is the instantaneous crystallization rate as a function of time at a given conversion α. According to this method, α function

TABLE 2 Avrami's parameters for the non-isothermal of pure PCL and nanocomposites

ϕ	5		10		20		30	
Samples	*n*	Z_c	*n*	Z_c	*n*	Z_c	*n*	Z_c
PCL	2.6	0.004	2.7	0.038	2.8	0.323	2.5	0.549
PCL + 1% Bent	2.5	0.005	2.4	0.109	2.4	0.380	2.2	0.575
PCL + 1% A	2.6	0.006	3.2	0.054	3.2	0.295	2.9	0.500
PCL + 1% B	3.0	0.003	3.2	0.055	3.0	0.323	3.1	0.478
PCL + 1% C	3.4	0.001	3.6	0.040	3.5	0.257	3.1	0.501
PCL + 2% Bent	2.3	0.008	2.4	0.110	2.4	0.389	2.3	0.575
PCL + 2% A	3.5	0.008	3.6	0.036	3.7	0.229	3.1	0.501
PCL + 2% B	2.9	0.003	3.4	0.044	3.0	0.275	2.8	0.524
PCL + 2% C	3.7	0.0006	3.9	0.031	3.9	0.234	3.8	0.407

TABLE 4 Activation energies of studied materials at three different crystallinity and nucleation activity

Crystallinity (%)	20	30	40	Nucleation activity
Samples	Activation energy (kJ/mol)			
PCL	121	98	90	1
PCL + 1% Bent	120	104	88	0.93
PCL + 1% A	142	116	108	0.84
PCL + 1% B	152	126	109	0.85
PCL + 1% C	142	116	92	0.82
PCL + 2% Bent	148	123	118	0.98
PCL + 2% A	153	126	98	0.77
PCL + 2% B	138	117	105	0.83
PCL + 2% C	153	123	94	0.86

obtained from the integration of the experimentally measured crystallization rates is initially differentiated with respect to time to obtain the instantaneous crystallization rate. Furthermore, by selecting appropriate degrees of crystallinity the values of $\partial\alpha/\partial t$ at a specific α (and measured at various cooling rate) are correlated to the corresponding crystallization temperature at this α (T_α). Then by plotting $\ln\partial\alpha/\partial t$, with respect to $1/T_\alpha$, a straight line must be obtained with a slope equal to $\Delta E_x/R$. Equation 7 was used only to make a qualitative comparison of the crystallization process between the matrix and nanocomposites. In this work, ΔE_x was evaluated at conversions of 0.2, 0.3, and 0.4, and the values are reported in Table 4. The results show that incorporation of bentonite to PCL matrix produced an increase on the activation energy which is in accordance with the previously observed retarding effect. No clear tendencies were observed as a function of SL and clay contents probably due to the different and competitive factors that affect to this parameter. Nevertheless, all used clays produce an increase in the activation energy and a reduction on the nucleation activity.

Figure 6 shows the continuous cooling transformations (CCTs), plots for the nanocomposites crystallization, where the crystallinity is related with time and temperature at constant cooling rate. This approach allows the knowledge of the crystallization process.[43,44] The curves for the relative degree of crystallinity (0.3) are plotted as a function of time. Theoretically, each point on these curves has been obtained by integration of the full model (nucleation and growth) at a constant cooling rate. So, when the degree of crystallization curve is intercepted by a constant cooling rate one, the obtained point represents the time necessary to reach a specific relative degree of crystallinity under specific thermal conditions. Figure 6A reveals that the Bent retards the crystallization process of PCL (crystallize at lower temperature and/or higher time), confirming the previously observed effect. On the other hand, the crystallization process was accelerated as a function of the content of SL. Similar behavior was observed in Figure 6B (with the exception of PCL and PCL + 2% A). It can be concluded that at higher contents, bentonite could affect the nucleating effect of SL.

4 | CONCLUSIONS

The effect of the incorporation of natural and SL-modified bentonite on the bulk crystallization of PCL was studied. Some relevant results (experimental and models parameters) demonstrated that natural unmodified bentonite nanoclays and bentonite modified with SL act as retarding agents but that SL is accelerating. Another important conclusion is that, although Avrami models and activation energy do not allow show appreciable differences between the different studied nanocomposites, the Mo models, nucleation activity, and CCT diagrams confirmed the previous analysis effects.

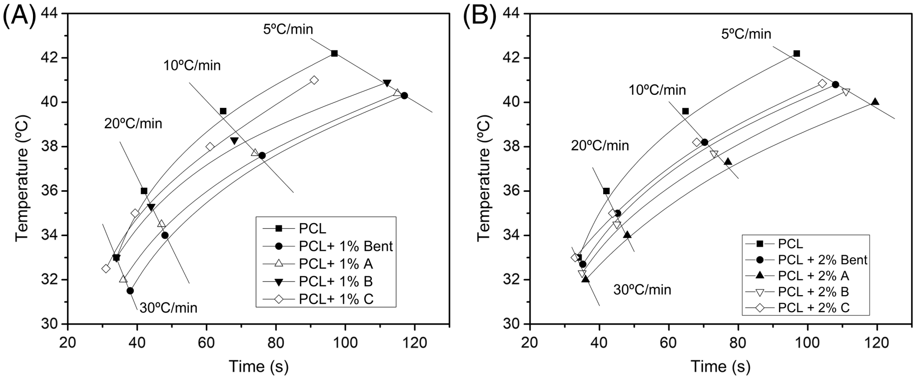

FIGURE 6 CCT diagrams for A, PCL and nanocomposites with 1% of each clay and B, PCL and nanocomposites with 2% of each clay

ACKNOWLEDGMENTS

The authors would like to acknowledge the financial support of the National Research Council of Argentina (CONICET) and the National Agency Promotion Scientific and Technological (ANPCyT).

ORCID

Claudio Javier Pérez http://orcid.org/0000-0003-1934-501X

REFERENCES

[1] R. Khankrua, S. Pivsa-Art, H. Hiroyuki, S. Suttiruengwong, *Energy Procedia* **2013**, *34*, 705.
[2] S. Ray, M. Okamoto, *Prog. Polym. Sci.* **2003**, *28*, 1539.
[3] Y. Di, S. Iannace, L. Sanguigno, L. Nicolais, *Macomol. Symp.* **2005**, *228*, 115.
[4] C. J. Perez, A. Vazquez, V. A. Alvarez, *J. Therm. Anal. Cal.* **2008**, *91*, 749.
[5] S. M. Davachi, B. S. Heidari, I. Hejazi, J. Seyfi, E. Oliaei, A. Farzaneh, H. Rashedi, *Carbohydr. Polym.* **2017**, *155*, 336.
[6] M. P. Guarás, V. A. Alvarez, L. N. Ludueña, *J. Appl. Polym. Sci.* **2016**, *133*(44). https://doi.org/10.1002/APP.44163.
[7] J. Kong, Y. Yu, X. Pei, C. Han, Y. Tan, L. Dong, *Int. J. Biol. Macromol.* **2017**, *102*, 1304.
[8] J. Iyer Ganapathi, F. T. Fisher, D. M. Kalyon, *J. Polym. Sci. Polym. Phys.* **2016**, *54*, 2254.
[9] F. Yahiaoui, F. Benhacine, H. Ferfera-Harrar, A. Habi, A. S. Hadj-Hamou, Y. Grohens, *J. Polym. Bull.* **2015**, *72*, 235.
[10] Q. Lu, C. Xu, D. Wu, Z. Wang, R. Lan, L. S. Wu, *Compos. Part A. Appl. Sci.* **2017**, *92*, 17.
[11] S. S. Ray, M. Bousmina, *Prog. Mater. Sci.* **2005**, *50*, 962.
[12] D. Merino, L. N. Ludueña, V. A. Alvarez, *J. Polym Environ* **2018**, *26*, 716.
[13] K. Saeed, S. Y. Park, *J. Appl. Polym. Sci.* **2007**, *104*, 1957.
[14] J. T. Yeh, M. C. Yang, C. J. Wu, C. S. Wu, *J. Appl. Polym. Sci.* **2009**, *112*, 660.
[15] T. M. Wu, E. C. Chen, *Polym. Eng. Sci.* **2006**, *46*, 1309.
[16] H. Liu, Y. Huang, L. Yuan, P. He, Z. Cai, Y. Shen, Y. Xu, Y. Yu, H. Xiong, *Carbohydr. Polym.* **2010**, *79*, 513.
[17] Q. Lu, C. Xu, D. Wu, Z. Wang, R. Lan, L. Wu, *Comp. Part A. Appl. Sci.* **2017**, *92*, 17.
[18] M. Lanfranconi, V. A. Alvarez, L. Ludueña, *J. Therm. Anal. Cal.* **2016**, *126*, 1273.
[19] Y. Huang, H. Liu, P. He, L. Yuan, H. Xiong, Y. Xu, *J. Appl. Polym. Sci.* **2010**, *116*, 2119.
[20] J. T. Xu, Y. Q. Zhao, Q. Wang, Z. Q. Fan, *Polymer* **2005**, *46*, 11978.
[21] P. Zou, S. Tang, Z. Fu, H. Xiong, *Int. J. Therm. Sci.* **2009**, *48*, 837.
[22] D. Merino, R. Ollier, M. Lanfranconi, V. Alvarez, *App. Clay Sci.* **2016**, *127*, 17.
[23] W. Y. Yam, J. Ismail, H. W. Kammer, H. Schmidt, C. Kummerlöwe, *Polymer* **1999**, *40*, 5545.
[24] L. Ludueña, A. Vazquez, V. Alvarez, *Carbohydr. Polym.* **2012**, *87*, 411.
[25] M. Pluta, A. Galeski, M. Alexandre, M. A. Paul, P. Dubois, *J. Appl. Polym. Sci.* **2002**, *86*, 1497.
[26] L. N. Ludueña, A. Vazquez, V. A. Alvarez, *J. Appl. Polym. Sci.* **2008**, *109*, 3148.
[27] C. J. Perez, V. A. Alvarez, *J. Therm. Anal. Cal.* **2016**, *124*, 499.
[28] V. P. Cyras, J. M. Kenny, A. Vazquez, *Polym. Eng. Sci.* **2001**, *41*, 1521.
[29] T. M. Wu, C. Y. Liu, *Polymer* **2005**, *46*, 5621.
[30] A. Sorrentino, R. Pantani, G. Titomanlio, *J. Polym. Sci. Polym. Phys.* **2007**, *45*, 196.
[31] S. A. E. Boyer, J. M. Haudin, *Polym. Test.* **2010**, *29*, 445.
[32] S. Boukettaya, W. Al Seddique, A. Alawar, H. Ben Daly, A. Hammani, *Sci. Eng. Comp. Mater.* **2016**, *23*, 523.
[33] M. L. Di Lorenzo, C. Silvestre, *Prog. Polym. Sci.* **1999**, *24*, 917.
[34] C. Jiao, Z. Wang, Z. Liang, Y. Hu, *Polym. Test.* **2005**, *24*, 71.
[35] C. J. Perez, V. A. Alvarez, *J. Appl. Polym. Sci.* **2009**, *114*, 3248.
[36] M. Avrami, *J. Chem. Phys.* **1940**, *8*, 212.
[37] A. Jeziorny, *Polymer* **1978**, *19*, 1142.
[38] C. J. Perez, V. A. Alvarez, *J. Therm. Anal. Cal.* **2016**, *124*, 499.
[39] V. A. Alvarez, C. J. Perez, *J. Therm. Anal. Cal.* **2012**, *107*, 633.
[40] T. X. Liu, Z. S. Mo, S. E. Wang, H. F. Zhang, *Polym. Eng. Sci.* **1997**, *37*, 568.
[41] A. Dobreva, I. Gutzow, *J. Non-Cryst. Solids* **1993**, *162*, 13.
[42] S. Vyazovkin, N. Sbirrazzuoli, *J. Phys. Chem. B.* **2003**, *107*, 882.
[43] J. Pruiell, J. White, *Polym. Eng. Sci.* **1975**, *15*, 660.
[44] C. Hsiung, M. Cakmak, J. White, *Int. Polym. Proc.* **1990**, *5*, 109.

How to cite this article: Merino D, Alvarez VA, Pérez CJ. Non-isothermal crystallization of poly(ε-caprolactone) nanocomposites with soy lecithin-modified bentonite. *Polymer Crystallization*. 2018;1:e10020. https://doi.org/10.1002/pcr2.10020